Available online at www.sciencedirect.com
SCIENCE DIRECT®
Colloids and Surfaces B: Biointerfaces 33 (2004) 211–226
COLLOIDS AND SURFACES B
www.elsevier.com/locate/colsurfb

A monolayer study on three binary mixed systems of dipalmitoyl phosphatidyl choline with cholesterol, cholestanol and stigmasterol

Munemori Kodama [a], Osamu Shibata [b], Shohei Nakamura [b], Sannamu Lee [a], Gohsuke Sugihara [a,*]

[a] *Department of Chemistry, Faculty of Science, Fukuoka University, Fukuoka 814-0180, Japan*
[b] *Department of Pharmaceutical Technology, Faculty of Pharmaceutical Science, Kyushu University, Fukuoka 812-8582, Japan*

Received 22 August 2003; accepted 1 October 2003

Abstract

The monolayer behavior of three mixed systems of dipalmitoyl phosphatidyl choline (DPPC) with sterols; cholesterol (Ch), stigmasterol (Stig), and cholestanol (Chsta) formed at the interface of air/water (phosphate buffer solution at 7.4 with addition of NaCl) was investigated in terms of surface pressure (π) and molecular occupation surface area (A) relation. A series of π–A curves at every 0.1 mol fraction of each sterol for the three combinations of mixed systems were obtained at 25.0 °C.

On the basis of the π–A curves, the additivity rule in regard to A versus sterol mole fraction (X_{st}) was examined at discrete surface pressures such as 5, 10, 15, 20, 25, 30 mN m^{-1}, and then from the obtained A–X_{st} curves the partial molecular areas (PMA) were determined. The A–X_{st} relation exhibited a marked negative deviation from ideal mixing in the pressure range below 10 mN m^{-1}, i.e. in the expanded liquid film region (below the transition pressure of DPPC).

The PMA of Ch at $\pi = 5$ mN m^{-1}, for example, was found to be conspicuously negative in the range of $X_{Ch} = 0$–0.2 (about -0.4 nm^2 per molecule) and slightly positive (ca. 0.1 nm^2 per molecule) in the range $X_{Ch} = 0.2$ to 0.4. Above $X_{Ch} = 0.5$, Ch's PMA was almost the same as the surface area of pure Ch, while DPPC's PMA was reduced to 60% of that of the pure system.

Excess Gibbs energy ($\Delta G_{(ex)}$) as a function of X_{st} was estimated at different pressures. Applying the regular solution theory to thermodynamic analysis of $\Delta G_{(ex)}$, the activity coefficients (f_1 and f_2) of DPPC and the respective sterols as well as the interaction parameter (I_p) in the mixed film phase were evaluated; the results showed a marked dependence on X_{st}.

Compressibility C_s and elasticity C_s^{-1} were also examined. These physical parameters directly reflected the mechanical strength of formed monolayer film.

Phase diagrams plotting the collapse pressure (π_c) against X_{st} were constructed, and the π_c versus X_{st} curves were examined for the respective mixed systems in comparison with the simulated curves of ideal mixing based on the Joos equation.

Comparing the monolayer behavior of the three mixed systems, little remarkable difference was found in regard to various aspects. In common among the three combinations, the mole fraction dependence in monolayer properties was classified into three ranges: $0 < X_{st} < 0.2$, $0.2 < X_{st} < 0.4$ and $0.5 < X_{st} < 1$. How the difference in the chemical structure of the sterols influenced the properties was examined in detail.

Keywords: Mixed monolayer; Dipalmitoyl phosphatidyl choline; Cholesterol; Cholestanol; Stigmasterol; Partial molecular area; Excess Gibbs energy; Interaction parameter

1. Introduction

As is well known that cell membrane composition directly participates in performance of different functions in close cooperation of such lipids as different phospholipids and sterols with various membrane proteins which exist together. Needless to say, the cell membranes are the so-called mixed systems and the structure constructed is not monolayer but bilayer. In order to examine the properties of bilayers comprising of mixtures of different types of ammphiphilic substances, monolayer studies can give us fundamental but indispensable information about such mixed systems. As a matter of fact, the monolayer behavior of many such mixtures has been investigated as functions of chemical species structure and their mixing ratios [1–8]. Due to the physicochemical importance of cholesterol (Ch) molecules in cell membrane, the interaction between Ch and other

* Corresponding author. Fax: +81-92-865-6030.
E-mail address: sugihara@cis.fukuoka-u.ac.jp (G. Sugihara).

0927-7765/$ – see front matter © 2003 Elsevier B.V. All rights reserved.
doi:10.1016/j.colsurfb.2003.10.008

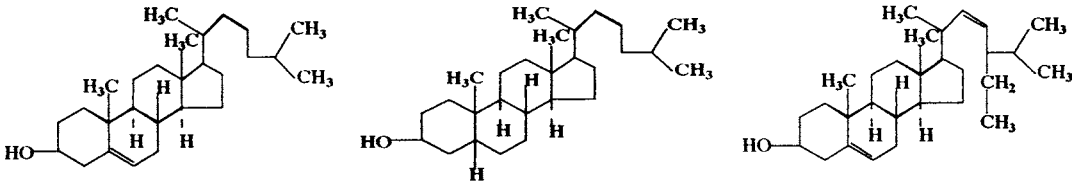

Scheme 1. Cholesterol cholestanol stigmasterol.

lipids has been studied by various physicochemical methods [5,9–11]. On the other hand, phospholipids have attracted a great attention because they are one of the most abundant ingredients in cell membranes [7]. The interaction between sphingomyelin as one phospholipid and Ch in biological and model membranes has been examined [12], following previous two studies: (i) based on the question: whether Ch can discriminate between sphingomyelin and phosphatidylcholine (PC) in mixed monolayers containing both phospholipids [13], and (ii) whether lateral domain formation in Ch/phospholipid monolayers is affected by the sterol side chain conformation [14]. The formation of condensed or multiple complexes of Ch and phospholipids in membrane (monolayers and bilayers) has been experimentally [15] and theoretically [16] studied, and the relationship between condensed complexes in monolayers and bilayers was discussed [16].

Among the many different phospholipids, 1,2-diphalmitoyl-sn-glycero-3-phosphatidylcholine (DPPC) has been in many cases employed for mixed monolayer studies [10,13,14,17,18]. We have previously examined the monolayer behavior of mixed systems of DPPC with hydrocarbon and fluorocarbon fatty acids; from it the conclusion that the interaction of DPPC with fluorocarbon fatty acids is stronger than that with hydrocarbon ones was reached [19]. Based on our interest in the pulmonary surfactant, we reported a study on dynamic surface properties of a synthesized peptide as a model membrane protein showing a lung surfactant-like activity in mixed monolayer with phospholipids, DPPC and egg phosphatidylcholine. It is noted that the peptide called Hel 13-5 [N- and C-termini amphiphilic α-helical peptide] is composed of twelve leucine (L), one tryptophan (W) and five lysine (K) residues [20].

According to Chou and Chang [18], in the alveolus, where the gas exchange takes place as one breathes, there are surface tension effects due to the extremely large air/aqueous interface. Natural pulmonary surfactant consists of approximately 10% protein and 90% lipids with DPPC as the most abundant component [21]. An important function of pulmonary surfactant is to reduce the surface tension of the air/aqueous interface in the alveolus, which is accompanied by the formation of a monolayer at the interface [22]. The monolayer is compressed and expanded successively during breathing, and acts to adjust the surface tension dynamically [23,24]. This specific interfacial property of lung surfactant enables it to decrease the work of breathing, prevent alveolar collapse at the end of expiration, and further reduce the driving force required for fluid to move into alveolar spaces [25]. On the basis of such knowledge on lung surfactant as mentioned here, in 2000 Chou and Chang reported a study on the thermodynamic behavior and relaxation process of mixed DPPC/Ch monolayers at the air/water interface [18]: this literature will be repeatedly quoted in the present paper for comparison.

Turning our attention to sterols as a counterpart of the three binary mixed systems with DPPC, as shown in Scheme 1, in addition to Ch, stigmasterol (Stig) as one of phytosteols (plant sterols, abundant in fat-soluble fractions of plants) and cholestanol (Chsta) as one of the phytostanols were chosen in order to compare the properties of the mixed films, some differences of which might come from the difference in their chemical structure. When phytosterols or phytostanols coexist with Ch in foodstuffs the formers are known to inhibit the absorption of Ch or reduce plasma total and low-density liporotein (LDL) Ch levels [26]. We have reported a thermodynamic study on selective solubilization among Ch, Stig and Chsta from their 1:1 mixtures by bile salt micelles in water. From this study marked effects of structural difference on solubilization were found, suggesting that the structure of micelles mixed with solubilizate as well as the interaction between solibilizates and solubilizers is varied with the differences in hydrophobic side chain and in the steric structure of the B–C–D rings of steroid skeleton [27]. This observation in addition to our interest in developing an artificial lung surfactant, has motivated us to investigate the mixed monolayers of DPPC with Ch, Stig and Chsta.

In this study, based on the curves of surface pressure (π) versus molecular surface area (A) obtained at every 0.1 mole fraction of each sterol for the three mixed systems, various thermodynamic analyses were carried out.

2. Materials and methods

2.1. Materials

Dipalmitoyl phosphatidyl choline (DPPC, >99%) was purchased from Avanti Polar-Lipids, Inc., cholesterol (>99%) from Sigma., cholestanol from Lancaster Synthesis,

and stigmasterol from Tama Biochemical Co. Ltd. These samples were used without further purification. Hexane and ethanol from Nacalai Tesque (Japan) were of analytical grade and used as received. Phosphate buffer solution was prepared using di-sodium hydrogenphosphate 12-water (Nacalai Tesque) and sodium dihydrogenphosphate dihydrate (Nacalai Tesque). Sodium chloride (Nacalai Tesque) was roasted at about 700 °C for 24 h to remove surface active impurities, before use as added salt.

2.2. Preparation of samples and subphase

Ch, Chsta, Stig and DPPC were dissolved separately in solvent mixtures of hexane and ethanol (9:1, v/v). They were mixed so as to have a desired composition of sterols for the three combinations of: DPPC/Ch, DPPC/Chsta, and DPPC/Stig. The prepared sample solutions were stored at about –5 °C.

The substrate solution, phosphate buffer saline(pH 7.4),was prepared using thrice distilled water with addition of sodium chloride (0.05 M) and phosphate buffer solution (0.1 M) [20].

2.3. Method

To obtain surface pressure (π)–area (A) curves, an automated balance using Willhelmy plate method (FSD-110, USI System Co. Ltd., Japan) equipped with a π–A curve recording system was used. The trough (35.3 cm × 10 cm × 0.5 cm) made from Teflon was washed with acetone and chloroform to remove all extraneous matter before each measurement. The two barriers were washed in a similar manner. Washing of glass equipment to remove any impurities was carried out using KOH/ethanol mixed solution [12]. The cleaning of the trough and subphase was carried out before each measurement by making the barriers approach each other to a distance of 3–5 mm to gather up any dust present and then using an aspirater, the dust was sucked up. Until an error margin within $\pm 0.2\,\mathrm{mN\,m^{-1}}$ was maintained during the compression of the entire surface by the two barriers, the cleaning was repeated. Each 30 μl of sample solution was then spread on the subphase with a Hamilton microsyringe, and 15 min were allowed for the solvent to evaporate before each run was started. The formed monolayer was compressed at the speed of about $0.05\,\mathrm{nm^2\,min^{-1}}$ per molecule. The measurement temperature was kept at 25 ± 0.2 °C (the room temperature was also kept at 25 ± 1.0 °C).

3. Result and discussions

3.1. π–A curves at discrete mole fractions

Fig. 1 shows π–A curves of DPPC/Ch mixed monolayers at various mole fractions of Ch. In Fig. 1, the π–A curve of the single system of DPPC demonstrates that π starts to go up

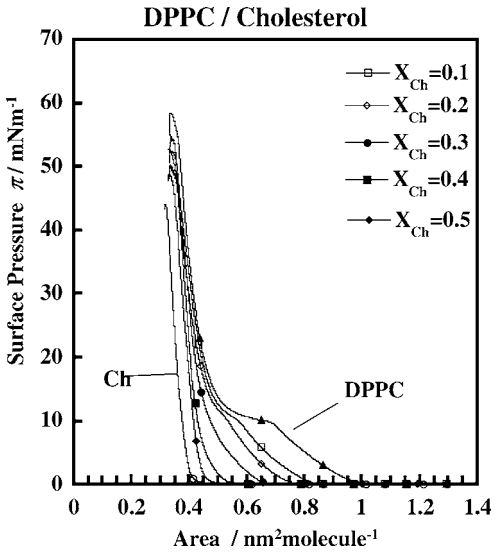

Fig. 1. π–A curves at discrete mole fractions of DPPC/Ch mixed monolayers at 298 K. (Crowded curves obtained for the mixtures above $X_{Ch} > 0.6$ are not shown here.)

with compression at the limiting surface area $a_0(DPPC) = 0.482\,\mathrm{nm^2}$ per molecule and reach a break point where a phase transition from liquid expanded state (LE) to liquid condensed state (LC) takes place ($\pi = 9.82\,\mathrm{mN\,m^{-1}}$, $A = 0.688\,\mathrm{nm^2}$ per molecule). These characteristic values are in good agreement with those of the literature ([28], vol. 1) [29]. It is noted, here, that no transition point was found on the π–A curve of DPPC single system on pure water subphase at 37 °C [18]. On the other hand, an abrupt increase in π was observed for the single system of Ch at the limiting surface area $a_0(\mathrm{Ch}) = 0.381\,\mathrm{nm^2}$ per molecule. This a_0 value as well as the collapse pressure determined at the breaking of the π–A curve is also in accordance with the literature ([28], vol. 2). The rapid increase of π suggests that the monolayer of Ch single system is more highly condensed than that of pure DPPC.

For the mixed systems, the π–A curves were obtained at every 0.1 mole fraction of Ch and in the figure curves up to $X_{Ch} = 0.5$ are given while those above $X_{Ch} = 0.6$ are so crowded that those are not shown. All of the curves of the mixed system appeared in the order of increase in mole fraction between those of both single systems. The break upon transition from LE to LC was observable up to $X_{Ch} = 0.2$, while such a transition point was not found for the DPPC/Ch system on water at 37 °C [18].

Fig. 2 shows π–A curves of DPPC/Chsta mixed monolayers at various mole fractions of Chsta. Compared with the π–A curve of pure Ch shown in Fig. 1, no remarkable difference was seen for pure Chsta π–A curve. In Fig. 2, the π–A curves for the mixed systems obtained at $X_{Chsta} = 0.1$ to 0.5 are included, and similar to the case of DPPC/Ch mixtures, those above $X_{Chsta} = 0.6$ are not shown because of overcrowding. At the lower surface pressure range, all the curves of the mixed systems are arrayed in the order of

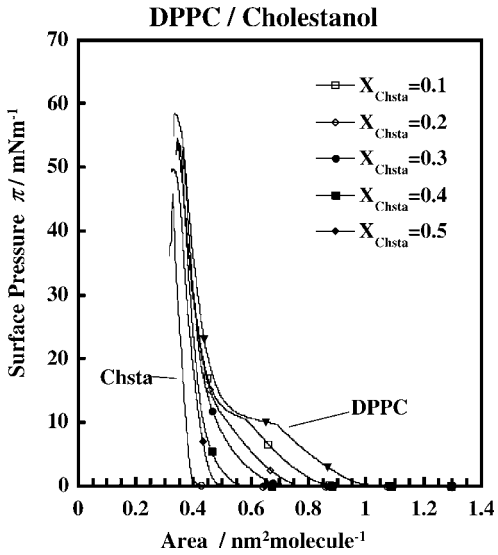

Fig. 2. π–A curves at discrete mole fractions of DPPC/Chsta mixed monolayers at 298 K. (Crowded curves obtained for the mixtures above $X_{\mathrm{Chsta}} > 0.6$ are not shown here.)

mole fraction. As for the transition point, a trend similar to DPPC/Ch was observed.

As shown in Fig. 3, the π–A curves were obtained for the Stig single system and the DPPC/Stig mixed systems at every 0.1 mole fraction (only the curves at 0.1–0.5 are given in the figure). Note that, compared with Ch and Chsta single systems, Stig has a lower collapse pressure. This may be caused by the larger area of the hydrophobic group next to the steroid skeleton which probably results in a reduction of cohesion among molecules. The lower collapse pressure coming from weaker interactive cohesion does not correspond to the difference in melting point (Ch = 149 °C, Chsta = 142 °C and Stig = 170 °C). The two-dimensional interaction among molecules floating at water surface seems to be different from that in three dimensional crystalline structure.

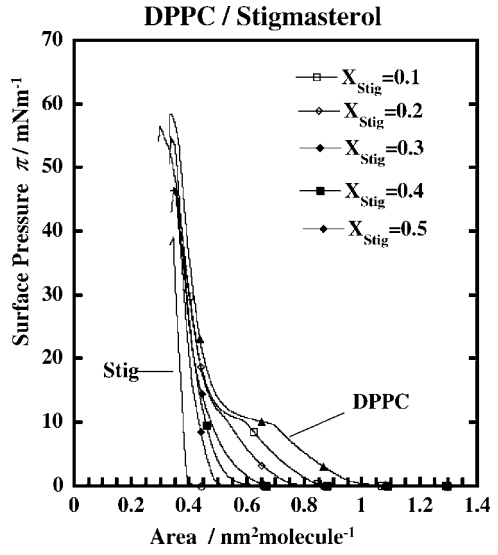

Fig. 3. π–A curves at discrete mole fractions of DPPC/Stig mixed monolayers at 298 K. (Crowded curves obtained for the mixtures above $X_{\mathrm{Stig}} > 0.6$ are not shown here.)

Looking at every curve shown Figs. 1–3, it is seen that the limiting surface area, a_0, depends greatly on composition at least in the region of sterol mole fraction from 0 to 0.5, while in the crowded region of π–A curves little dependence is observed. This suggests that the properties of monolayers of the present three mixed systems are in common governed by whether each sterol is a minor component ($X_{\mathrm{st}} < 0.5$) or a major one ($X_{\mathrm{st}} > 0.5$) and the interaction mode of DPPC with sterols is distinctly different above and below $X_{\mathrm{st}} = 0.5$. (This fact will be confirmed by the following analyses.) It is noted that Chou and Chang found the existence of a boundary at $X_{\mathrm{Ch}} = 0.4$ for DPPC/Ch system at 37 °C in terms of various properties such as area per molecule (A) or excess area (A_{ex}), excess free energy ($\Delta G_{(\mathrm{ex})}$) and free energy of mixing (ΔG_{mix}) [18].

The transition pressure specific to DPPC, π_{t}, is observable up to $X_{\mathrm{st}} = 0.2$ for all three mixtures. The collapse pressure, π_{c}, was also approximately determinable, although the π_{c} for mixed systems has to some extent a large error margin, in particular, in the higher range of X_{st}.

In addition to a_0, π_{c} and π_{t} data are also tabulated in Table 1 as a function of mole fraction of sterol.

3.2. Mean molecular surface areas (A_m) and partial molecular areas (PMA)

When π–A curves of a given binary mixture are analyzed, it is essential to examine whether the relation of mean molecular (surface) area (A_{m}) with mole fraction (X) has a linear relation satisfying the additivity rule or not, and if not so, whether negative or positive deviations are observed.

In Fig. 4(A), the A_{m} for the DPPC/Ch mixed system is plotted against X_{Ch} at discrete surface pressures, 5, 10, 15, 20, 25 and 30 mN m^{-1}, and similarly the A_{m} versus X_{st} relations are shown for the DPPC/Chsta and DPPC/Stig mixed systems in Fig. 4(B and C), respectively. Either a mixed system can form ideally mixed monolayer or cannot mix completely but can form the so-called patched film; the additivity should show a linear relation as indicated by a broken line. All the mixed systems, as shown in Fig. 4(A–C), demonstrate that at lower pressures such as 5 and 10 mN m^{-1}, a marked negative deviation is shown, especially below $X_{\mathrm{st}} = 0.5$. Fig. 4 also tells us that the π–A behavior is divided into two distinct ranges; below and above $X_{\mathrm{st}} = 0.5$. (Otherwise we may say "below and above $X_{\mathrm{st}} = 0.4$" as Chou and Chang said [18]).

The surface occupation behavior can be more clearly seen if the partial molecular area is evaluated, as has been employed in previous studies [19,20]. In the frame for π = 5 mN m^{-1} of Fig. 4(D), two examples of how to determine

Table 1
Basic π–A data

Mole fraction, X	Limiting area, a_0 (nm^2 per molecule)	Transition point		Collapse pressure, π (mN m^{-1})
		π (mN m^{-1})	A (nm^2 per molecule)	
(a) DPPC/Ch mixed system				
0.0	0.482	9.82	0.688	54.4
0.1	0.484	10.23	0.571	45.3
0.2	0.453	10.83	0.517	
0.3	0.448			47.1
0.4	0.437			44.0
0.5	0.431			43.8
0.6	0.427			42.1
0.7	0.425			43.4
0.8	0.405			41.6
0.9	0.383			41.3
1.0	0.381			43.2
(b) DPPC/Chsta mixed system				
0.0	0.482	9.82		54.4
0.1	0.464	10.43		
0.2	0.441	10.84		
0.3	0.442			47.1
0.4	0.422			48.3
0.5	0.425			45.4
0.6	0.417			45.8
0.7	0.413			46.9
0.8	0.406			45.3
0.9	0.385			46.4
1.0	0.373			45.6
(c) DPPC/Stig mixed system				
0.0	0.482	9.82	0.688	54.4
0.1	0.485	10.23	0.588	46.6
0.2	0.445	10.84	0.518	40.7
0.3	0.453			39.7
0.4	0.452			41.5
0.5	0.430			42.2
0.6	0.425			40.9
0.7	0.427			39.9
0.8	0.422			39.5
0.9	0.397			38.1
1.0	0.388			38.8

the PMAs, i.e., $\bar{A}_1$ and $\bar{A}_2$ from the relation is given as

$$A_m = \bar{A}_1 + X_2 \left(\frac{\partial A_m}{\partial N_1} \right)_{T,V,\pi,N_2(j \neq i)} \quad (1)$$

$\bar{A}_1$ is here, the PMA of component 1 and defined as:

$$\bar{A}_1 = \left(\frac{\partial A_t}{\partial N_1} \right)_{T,V,\pi,N_2}$$

when N_1 plus N_2 molecules form a surface area A_t ($N_1\bar{A}_1 + N_2\bar{A}_2 = A_t$, and 1 and 2 denote DPPC and each sterol, respectively).

The term of partial derivative corresponds to the tangential slope at a point on the A_m versus X_2 curve, and the intercepts of both side ordinates can give $\bar{A}_1$ and $\bar{A}_2$, respectively [19].

Again looking at Fig. 4(D) at $\pi = 5\,\mathrm{mN\,m^{-1}}$: (i) in the range from $X_{Ch} = 0$ to 0.2, the tangential curve gives Ch a markedly great negative value as $\bar{A}_{Ch} \simeq -0.4\,\mathrm{nm^2}$ per molecule, (ii) in the range of $X_{Ch} = 0.2$ to 0.4 PMA is estimated as ca. $0.1\,\mathrm{nm^2}$ per molecule and (iii) in the region above $X_{Ch} = 0.5$, since the relation is approximately linear, $\bar{A}_{Ch}$ is the same as that of pure Ch (A^0_{Ch}), while $\bar{A}_{DPPC}$ is ca $0.48\,\mathrm{nm^2}$ per molecule. Interestingly, in the range above $X_{Ch} = 0.5$, DPPC shows to have a 40% reduced PMA while Ch keeps its PMA constant. Thus, the trend seen above $X_{Ch} = 0.5$ seems to be true for that at higher surface pressures. (Fig. 4 (D) is for DPPC/Stig mixture).

On the other hand in the range below $X_{Ch} = 0.5$, i.e. in the case where Ch is a minor component, Ch changes its PMA very widely. It should be kept in mind that the PMA below $X_{Ch} = 0.2$ is negative. The PMA behavior of the other mixtures (see Fig. 4(B and C)) is summarized as follows. (i) In the range below $X_{st} = 0.2$: (a) At $\pi = 5\,\mathrm{mN\,m^{-1}}$, PMA: ca. $-0.3\,\mathrm{nm^2}$ per molecule for both of Chsta and Stig were obtained, while (b) at $10\,\mathrm{mN\,m^{-1}}$ PMAs are -0.05 for Chsta and $0.05\,\mathrm{nm^2}$ per molecule for Stig. With increased surface

pressure of 5 mN m^{-1} PMAs for sterols do increase as was described here, in contrast, the PMA for DPPC is the same as the molecular area of the pure system but its value decreases. (ii) In the range between $X_{st} = 0.2$ and 0.5: (a) At $\pi = 5$ mN m^{-1}, PMAs for Chsta and Stig are 0.05 and 0 nm^2 per molecule, respectively, while the PMA for DPPC is reduced to 0.75 nm^2 per molecule (by about 0.05 nm^2 per molecule) in DPPC/Chsta as well as DPPC/Stig mixtures. (b) At $\pi = 10$ mN m^{-1} PMAs are estimated as 0.18 nm^2 per molecule for Chsta and 0.32 nm^2 per molecule for Stig, the PMA for DPPC is 0.6 nm^2 per molecule in DPPC/Chsta and is 0.55 nm^2 per molecule in DPPC/Stig mixed systems. In this composition range, the PMAs of both DPPC and the sterol mixtures are smaller than those of the respective single systems. (iii) In the range around $X_{st} = 0.5$: comparison of the curves around this mole fraction shows the curvature is different depending on the species; this seems to reflect the slight difference in chemical structure of the sterols. However, any further discussion done by relating to their chemical structure is impossible at present. (iv) In the

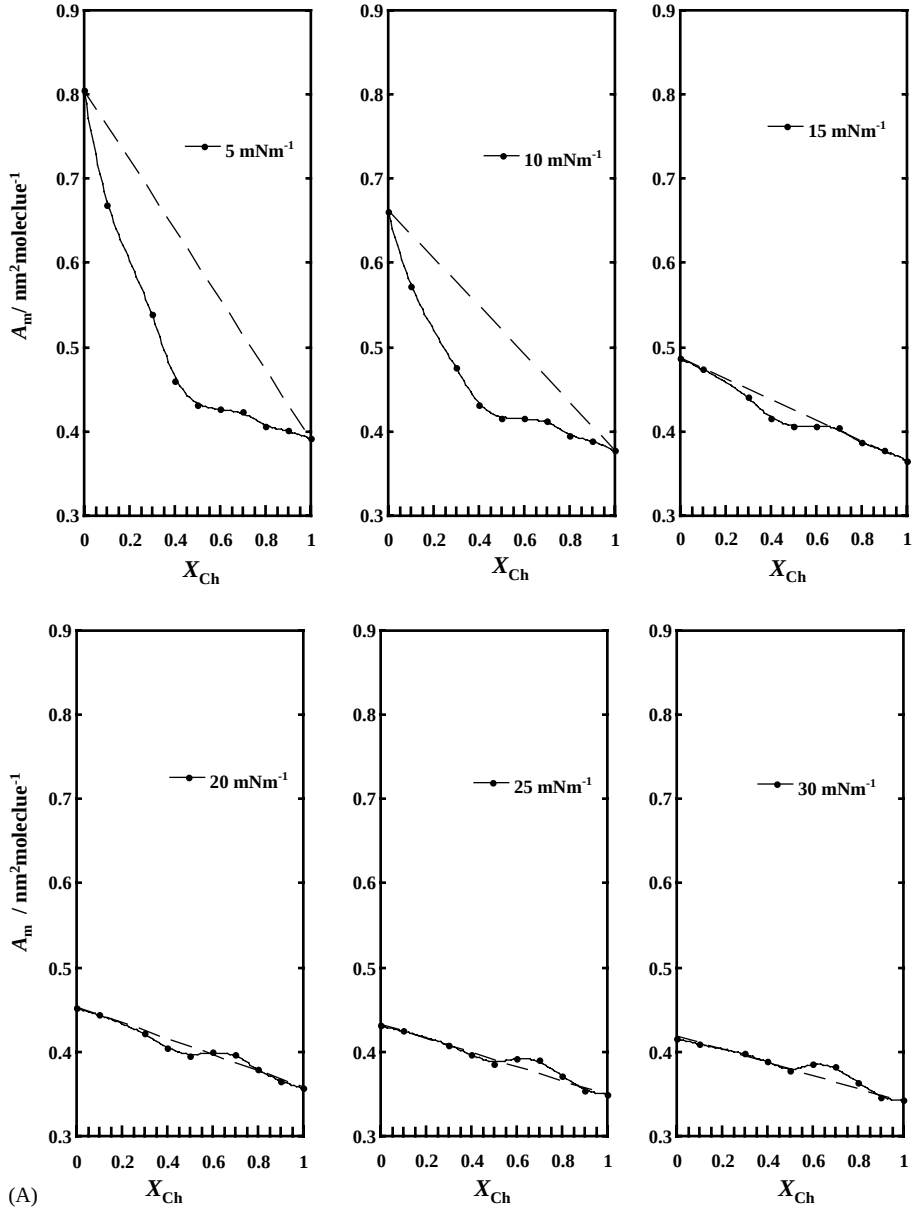

(A)

Fig. 4. (A) Molecular occupation surface area in the DPPC/cholesterol mixed systems at discrete surface pressures at 298 K. Note that the partial molecular area (PMA) of cholesterol at $\pi = 5$ mN m^{-1} is markedly negative at $X_{Ch} = 0$–0.2 (about -0.4 nm^2 per molecule), and at $X_{Ch} = 0.2$ to 0.4 PMA is estimated as ca. 0.1 nm^2 per molecule. (B) Molecular occupation surface area in the DPPC/cholestanol mixed systems at discrete surface pressures at 298 K. (C) Molecular occupation surface area in the DPPC/stigmasterol mixed systems at discrete surface pressures at 298 K. (D) Examples showing how to determine PMAs for DPPC/Stig mixture.

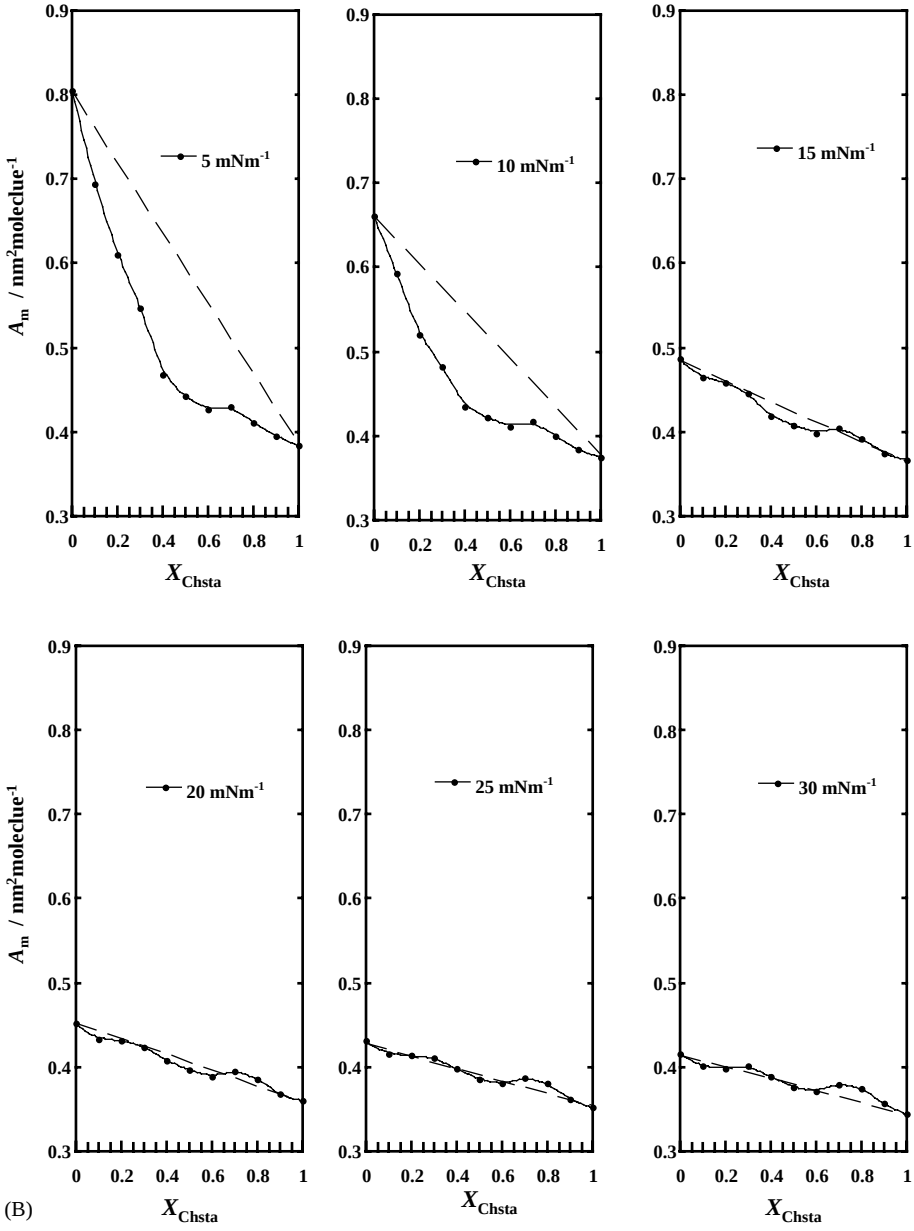

Fig. 4. (*Continued*).

sterol-rich range: DPPC/Chsta as well as DPPC/Stig mixed system shows almost linear relation at both pressures, indicating that the PMA of sterols is the same as that of each pure system, while DPPC contracts its PMA.

In common with DPPC/Ch, DPPC/Chsta and DPPC/Stig mixed systems have shown such characteristic PMA changes depending greatly much on the composition range as mentioned above. Here, it is noted that the interesting negative PMA means that addition of a molecule to a given monolayer system causes a reduction in total area as much as the value of negative the PMA, or accompanying the introduction of a molecule into the given surface, the interaction among molecules is enhanced.

The present discussion was restricted to the PMA behavior below $\pi = 10\,\mathrm{mN\,m^{-1}}$; this pressure is just below the transition point of DPPC. The characteristic PMA behavior may be directly related to the expanded liquid state of DPPC. In the DPPC-rich region, DPPC can intake very easily the added sterol molecules with neither contraction of DPPC molecules themselves no further expansion. On the other hand in the sterol-major region, sterols accept easily DPPC molecules the surface of which is reduced by counter-part sterols. It can be said that flexibility is sufficiently displayed in conformation change in the liquid expanded monolayer phase.

In contrast, at the higher surface pressure, where DPPC molecules form a condensed liquid film, all of the three mix-

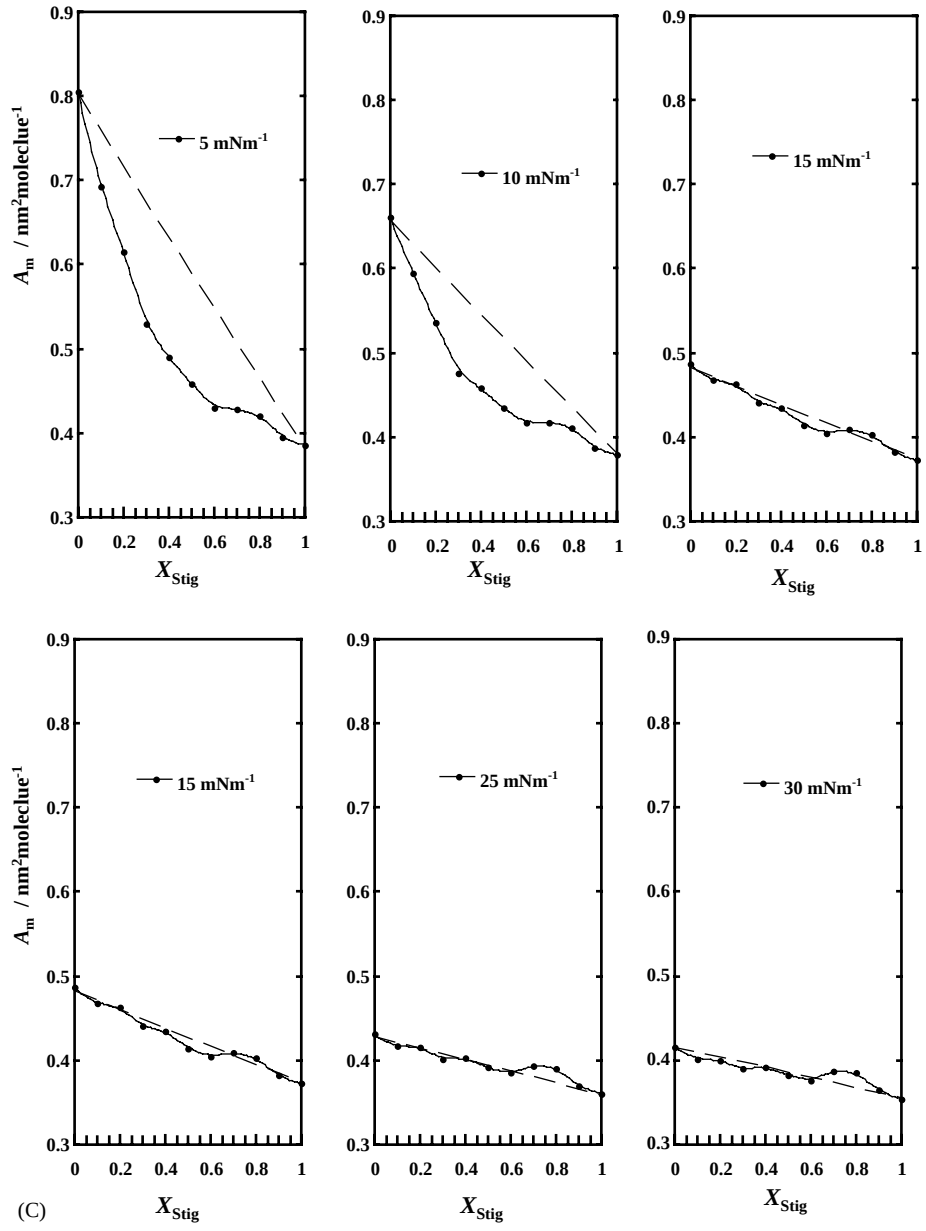

Fig. 4. (*Continued*).

tures show an almost linear relation in regard to A_m versus X_{st} plots, although small negative or positive deviations from the additivity rule are seen. However, these deviations are not attributable to either experimental errors or any significant change.

3.3. Thermodynamic analysis of the excess Gibbs energy

As a powerful tool for evaluating the interaction among molecules in the formed monolayer comprising two or more components and its thermodynamic stability, the surface excess Gibbs energy, $\Delta G_{(ex)}$, can be used as followings [1,18]. The Gibbs energy change upon mixing of species 1 and 2, ΔG_{mix} for a real mixed system, is considered to be a sum of ideal and excess Gibbs energy changes as $\Delta G_{mix} = \Delta G_{(id)} + \Delta G_{(ex)}$. For ideal mixing the Gibbs energy change involves only the entropy term as $\Delta G_{(id)} = RT(X_1 \ln X_1 + X_2 \ln X_2)$, where $X_i\,(i = 1, 2)$ denotes mole fraction in the mixture and R is the gas constant times Kelvin temperature. Further, the excess Gibbs energy can be expressed as:

$$\Delta G_{(ex)} = \int_0^{\pi} [A_{12} - (X_1 A_1 + X_2 A_2)]\,\mathrm{d}\pi \qquad (2)$$

where A_{12}, A_1, and A_2 represent the area of mixed system and the respective areas of components 1 and 2, and π is the surface pressure. It is noted that if the monolayer is an ideally mixed one, $\Delta G_{(ex)}$ is zero because A_{12} should be

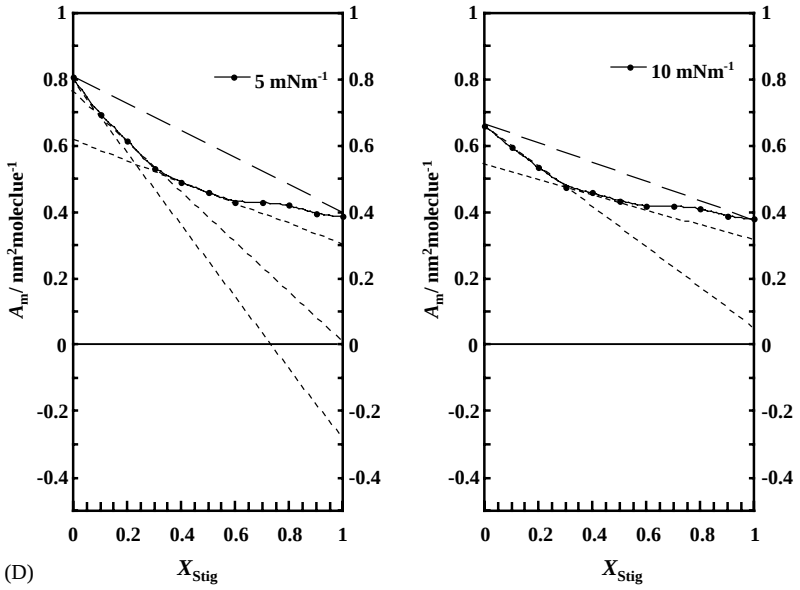

Fig. 4. (*Continued*).

equal to $(X_1A_1 + X_2A_2)$ corresponding to the additivity rule [18,30] (Table 2).

Three frames in Fig. 5 shows the $\Delta G_{(ex)}$ as a function of mole fraction of the respective sterols at a few selected pressures (5, 10 and 25 mN m^{-1}). $\Delta G_{(ex)}$ was calculated on the basis of Eq. (2). Comparing the curves, first of all, as a function of pressure for three mixed systems, the $\Delta G_{(ex)}$ value becomes, in common, lower (more negative) with increased surface pressure and shows a minimum at $X_{st} = 0.4$ (except for Stig) up to $\pi = 15$ mN m^{-1} but the minimum shifts toward $X_{st} = 0.5$ at pressures higher than 20 mN m^{-1} (curves for up to 30 mN m^{-1} were obtained but are not shown here). In regard to the deepness of the minima, this decreases in the order of DPPC/Ch, DPPC/Chsta, and DPPC/Stig, suggesting that thermodynamic stability of the monolayers becomes less in this order. All the data of the excess Gibbs energies determined at discrete pressures for the three combinations are tabulated in Table 3(a–c). It is noted that the absolute values of $\Delta G_{(ex)}$ at the lower mole fractions of sterols ($X_{st} = 0.1$–0.3) are, in general, found to be greater than those at the higher mole fraction ($X_{st} = 0.7$–0.9). A similar trend showing a minimum at $X_{Ch} = 0.4$ or $X_{DPPC} = 0.6$ has been reported for the DPPC/Ch mixed system at 37 °C [18], although the absolute value itself is different because of the difference in temperature.

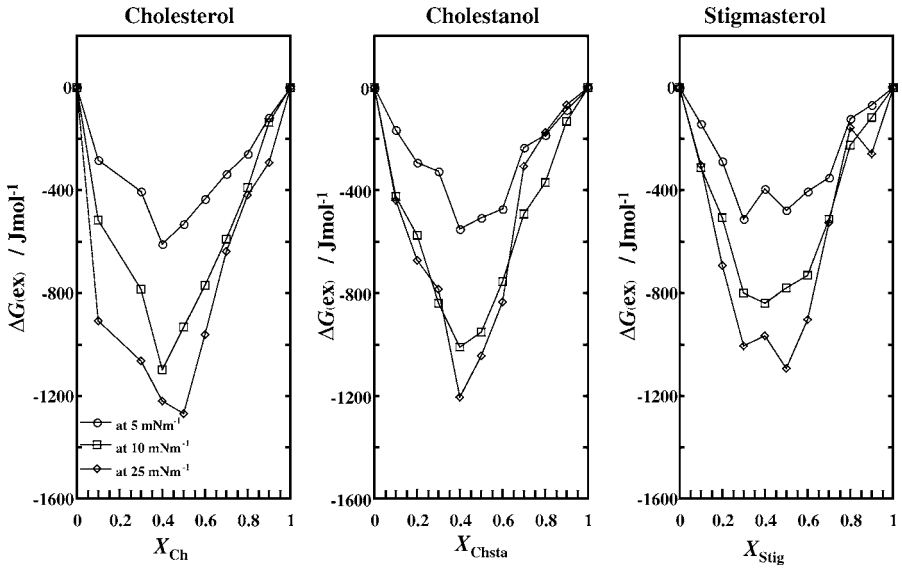

Fig. 5. Excess Gibbs energy as a function of mole fraction of sterols in the mixed monolayers at fixed surface pressure at 298 K.

Table 2
Mean molecular surface area as a function of mole fraction of sterols at discrete surface pressures

Mole fraction, X	Mean surface molecular area					
	$\pi = 5\,\mathrm{mN\,m^{-1}}$	$\pi = 10\,\mathrm{mN\,m^{-1}}$	$\pi = 15\,\mathrm{mN\,m^{-1}}$	$\pi = 20\,\mathrm{mN\,m^{-1}}$	$\pi = 25\,\mathrm{mN\,m^{-1}}$	$\pi = 30\,\mathrm{mN\,m^{-1}}$
(a) DPPC/Ch mixed system						
0.0	0.805	0.660	0.486	0.451	0.430	0.415
0.1	0.668	0.572	0.473	0.443	0.424	0.409
0.2	0.610	0.520	0.459	0.431	0.413	0.398
0.3	0.539	0.475	0.440	0.421	0.408	0.397
0.4	0.459	0.431	0.415	0.405	0.396	0.388
0.5	0.431	0.416	0.405	0.395	0.386	0.377
0.6	0.426	0.414	0.406	0.399	0.392	0.385
0.7	0.423	0.412	0.404	0.396	0.389	0.382
0.8	0.405	0.394	0.386	0.378	0.371	0.364
0.9	0.400	0.388	0.377	0.365	0.354	0.345
1.0	0.391	0.377	0.365	0.357	0.349	0.342
(b) DPPC/Chsta mixed system						
0.0	0.805	0.660	0.486	0.451	0.430	0.415
0.1	0.695	0.593	0.464	0.433	0.416	0.401
0.2	0.610	0.520	0.458	0.431	0.413	0.398
0.3	0.547	0.482	0.445	0.424	0.411	0.401
0.4	0.467	0.435	0.418	0.407	0.398	0.389
0.5	0.442	0.422	0.408	0.396	0.385	0.376
0.6	0.427	0.411	0.398	0.389	0.380	0.372
0.7	0.430	0.416	0.405	0.395	0.386	0.379
0.8	0.410	0.400	0.392	0.386	0.380	0.374
0.9	0.395	0.383	0.374	0.367	0.361	0.356
1.0	0.383	0.374	0.367	0.360	0.352	0.343
(c) DPPC/Stig mixed system						
0.0	0.805	0.660	0.486	0.451	0.430	0.415
0.1	0.693	0.594	0.467	0.435	0.417	0.401
0.2	0.615	0.535	0.463	0.434	0.415	0.400
0.3	0.529	0.476	0.440	0.417	0.401	0.389
0.4	0.490	0.457	0.434	0.416	0.403	0.392
0.5	0.458	0.434	0.414	0.401	0.391	0.382
0.6	0.430	0.417	0.405	0.394	0.384	0.376
0.7	0.428	0.417	0.408	0.401	0.393	0.387
0.8	0.420	0.411	0.402	0.396	0.390	0.385
0.9	0.395	0.387	0.381	0.375	0.370	0.364
1.0	0.385	0.379	0.372	0.366	0.360	0.354

As for the excess Gibbs energy, a thermodynamic analysis may be developed in more detail, as follows.

Supposing, here, that the regular solution theory (RST) was approximately applicable to the present mixed systems, the real entropy term $-T\,\Delta S^{\circ}_{\mathrm{mix}}$ (real) can be regarded as equal to $-T\,\Delta S^{\circ}_{\mathrm{mix}}$ (ideal) [31]. Thus, it is considered that the excess Gibbs free energy change upon mixing is the same as the enthalpy term ($\Delta H^{\circ}_{\mathrm{mix}}$) itself. When the chemical potential of i ($i = 1, 2$) in monolayer is given as $\mu_i = \mu_i^{\circ} + RT \ln f_i X_i$, where μ_i° is the standard chemical potential and f_i is the activity coefficient, the $\Delta G_{(\mathrm{ex})}$ can be expressed as

$$\Delta G_{(\mathrm{ex})} = \Delta H^{\circ}_{\mathrm{mix}} = RT(X_1 \ln f_1 + X_2 \ln f_2) \tag{3}$$

the right hand side of this equation can be regarded as the same as the right hand side of Eq. (2). The activity coefficient f_i is known to reflect an intermolecular interaction, and according to RST, f_i is given as follows:

$$\ln f_1 = \frac{\omega(1 - X_1)^2}{RT}, \qquad \ln f_2 = \frac{\omega(1 - X_2)^2}{RT} \tag{4}$$

where ω is the interaction parameter which is ascribed to cohesive forces between unlike molecules [31,32]. From Eq. (4), the following relation is obtained.

$$\ln f_1 = \frac{(1 - X_1)^2}{X_1^2} \ln f_2 \tag{5}$$

Substituting Eq. (5) into Eq. (3), we have

$$\frac{\Delta G_{(\mathrm{ex})}}{RT} = \left(\frac{X_2^2}{1 - X_2} + X_2 \right) \ln f_2 \tag{6}$$

all the quantities of the left hand side are known (Table 3), and X_1 and X_2 on the right hand side are also known, so the activity coefficients f_1 and f_2 can be calculated [33]. In addition, following substitution of Eq. (4) into Eq. (3),

Table 3
Excess Gibbs energy as a function of mole fraction of sterols at discrete surface pressures

Mole fraction, X	Excess Gibbs energy ($\times 10^2$ J mol^{-1})					
	$\pi = 5$ mN m^{-1}	$\pi = 10$ mN m^{-1}	$\pi = 15$ mN m^{-1}	$\pi = 20$ mN m^{-1}	$\pi = 25$ mN m^{-1}	$\pi = 30$ mN m^{-1}
(a) DPPC/Ch mixed system						
0.0	0	0	0	0	0	0
0.1	−0.28	−0.52	−0.56	−0.57	−0.91	−0.88
0.2	−0.29	−0.58	−0.53	−0.80	−0.68	−0.85
0.3	−0.40	−0.79	−0.99	−0.91	−1.06	−1.19
0.4	−0.61	−1.10	−1.20	−1.20	−1.22	−1.40
0.5	−0.53	−0.93	−1.10	−1.25	−1.27	−1.46
0.6	−0.44	−0.77	−0.91	−0.85	−0.96	−0.82
0.7	−0.34	−0.59	−0.53	−0.48	−0.64	−0.62
0.8	−0.26	−0.39	−0.38	−0.32	−0.42	−0.65
0.9	−0.12	−0.14	−0.23	−0.18	−0.29	−0.40
1.0	0	0	0	0	0	0
(b) DPPC/Chsta mixed system						
0.0	0	0	0	0	0	0
0.1	−0.16	−0.42	−0.26	−0.46	−0.44	−0.72
0.2	−0.29	−0.58	−0.53	−0.80	−0.67	−0.85
0.3	−0.33	−0.84	−1.02	−0.89	−0.79	−1.01
0.4	−0.55	−1.01	−1.08	−1.22	−1.31	−1.29
0.5	−0.51	−0.95	−1.04	−1.23	−1.04	−1.37
0.6	−0.48	−0.76	−0.84	−1.00	−0.84	−0.96
0.7	−0.23	−0.49	−0.46	−0.64	−0.31	−0.59
0.8	−0.19	−0.37	−0.39	−0.53	−0.18	−0.37
0.9	−0.09	−0.13	−0.25	−0.37	−0.07	−0.18
1.0	0	0	0	0	0	0
(c) DPPC/Stig mixed system						
0.0	0	0	0	0	0	0
0.1	−0.14	−0.31	−0.46	−0.28	−0.31	−0.71
0.2	−0.29	−0.51	−0.59	−0.59	−0.70	−0.74
0.3	−0.51	−0.80	−1.01	−0.77	−1.01	−1.02
0.4	−0.40	−0.84	−0.93	−1.07	−0.97	−0.95
0.5	−0.48	−0.78	−0.84	−0.94	−1.09	−1.21
0.6	−0.41	−0.73	−0.76	−0.89	−0.90	−0.99
0.7	−0.35	−0.51	−0.57	−0.49	−0.53	−0.57
0.8	−0.12	−0.22	−0.30	−0.21	−0.16	−0.22
0.9	−0.07	−0.12	−0.09	−0.18	−0.26	−0.13
1.0	0	0	0	0	0	0

we can calculate the interaction parameter ω from the next equation [33]:

$$\omega = \frac{\Delta G_{(ex)}}{X_1 X_2} \tag{7}$$

The obtained values of $I_p = \omega/RT$ and the activity coefficients for the respective systems are listed in Tables 4 and 5. The I_p values are all negative as expected from the $\Delta G_{(ex)}$ values, and the greater values obtained are common for all the mixtures at almost all pressures at around $X_{st} = 0.4$–0.5. However, attention should be paid to the I_p values at 30 mN m^{-1} which are the greatest for all the mixtures at $X_{st} = 0.1$, suggesting a sterol molecule as the minority can interact most strongly with DPPC molecules as the majority. This situation is reflected by the activity coefficients. Comparing the f_1 (for DPPC) and f_2 (for sterols) values at $X_{st} = 0.1$, f_1 is very close to one (unity) while f_2 is very small; especially at $\pi = 30$ mN m^{-1} $f_1 = 0.96$ and 0.97 while $f_2 = 0.04$ and 0.07 for the DPPC/Ch and DPPC/Chsta mixtures, respectively.

3.4. Compressibility

For analysis of the properties of monolayer films, compressibility Cs or elasticity Cs^{-1} may be used as a measure. The characteristic curves of $(\partial\pi/\partial A)_T$ is related to compressibility

$$\mathrm{Cs} = -\frac{1}{A}\left(\frac{\partial A}{\partial \pi}\right)_T \tag{8}$$

where A and π are already defined area and surface pressure, respectively. The reciprocal of compressibility, Cs^{-1}, is equivalent to elasticity. Therefore, the maximum of the $-(\partial\pi/\partial A)$ curve corresponds to the maximum elasticity. In this paper, the mechanical property is described in terms of elasticity (Cs^{-1}). It has been known that Cs^{-1} value ranges

Table 4
The interaction parameter $I_p = \omega/RT$ as a function of mole fraction of sterols at discrete pressures

Mole fraction, X	Interaction parameter					
	$\pi = 5\,mN\,m^{-1}$	$\pi = 10\,mN\,m^{-1}$	$\pi = 15\,mN\,m^{-1}$	$\pi = 20\,mN\,m^{-1}$	$\pi = 25\,mN\,m^{-1}$	$\pi = 30\,mN\,m^{-1}$
(a) DPPC/Ch mixed system						
0.0						
0.1	−1.27	−2.32	−2.52	−2.54	−4.08	−3.94
0.2	−0.74	−1.46	−1.35	−2.02	−1.70	−2.13
0.3	−0.78	−1.51	−1.91	−1.74	−2.04	−2.29
0.4	−1.02	−1.85	−2.03	−2.02	−2.05	−2.34
0.5	−0.86	−1.51	−1.77	−2.02	−2.05	−2.35
0.6	−0.73	−1.30	−1.53	−1.43	−1.62	−1.38
0.7	−0.65	−1.14	−1.02	−0.91	−1.23	−1.20
0.8	−0.65	−0.99	−0.95	−0.80	−1.05	−1.64
0.9	−0.52	−0.61	−1.05	−0.78	−1.31	−1.76
1.0						
(b) DPPC/Chsta mixed system						
0.0						
0.1	−0.74	−1.90	−1.16	−2.06	−1.97	−3.22
0.2	−0.74	−1.46	−1.35	−2.02	−1.70	−2.13
0.3	−0.63	−1.61	−1.96	−1.70	−1.51	−1.93
0.4	−0.92	−1.70	−1.81	−2.06	−2.03	−2.17
0.5	−0.82	−1.53	−1.68	−1.99	−1.69	−2.21
0.6	−0.80	−1.27	−1.40	−1.68	−1.41	−1.61
0.7	−0.45	−0.95	−0.88	−1.23	−0.59	−1.14
0.8	−0.47	−0.94	−0.98	−1.34	−0.45	−0.93
0.9	−0.40	−0.58	−1.11	−1.64	−0.31	−0.81
1.0						
(c) DPPC/Stig mixed system						
0.0						
0.1	−0.63	−1.39	−2.07	−1.24	−1.34	−3.20
0.2	−0.73	−1.28	−1.49	−1.48	−1.75	−1.87
0.3	−0.98	−1.53	−1.94	−1.48	−1.93	−1.96
0.4	−0.67	−1.42	−1.56	−1.79	−1.62	−1.59
0.5	−0.78	−1.26	−1.36	−1.52	−1.77	−1.96
0.6	−0.68	−1.23	−1.27	−1.50	−1.52	−1.66
0.7	−0.67	−0.99	−1.09	−0.94	−1.01	−1.09
0.8	−0.31	−0.57	−0.76	−0.54	−0.40	−0.56
0.9	−0.30	−0.52	−0.42	−0.82	−1.16	−0.60
1.0						

from 10 to 50 mN m^{-1} for liquid expanded films and from 100 to 250 mN m^{-1} for liquid condensed film [34]. In Fig.6, Cs^{-1} values which were determined at different pressures are plotted as a function of sterol mole fraction for the three mixed systems (the results at 15, 20 and 30 mN m^{-1} are not shown in the figure to avoid complexity). Looking first of all at the value of single systems of sterol, Ch is the lowest and Stig is the highest at $\pi = 5\,mN\,m^{-1}$, while Ch is the lowest and Chsta is the highest at $\pi = 10\,mN\,m^{-1}$, suggesting Ch is more compressible than Chsta and Stig. Comparing the ranges of the liquid expanded films (whose Cs^{-1} values are below 50) among three mixtures at $\pi = 5\,mN\,m^{-1}$, DPPC/Ch seems to have a little wider range (up to $X_{Ch} = 0.45$) than the others (up to X_{Chsta} and $X_{stig} = 0.35$). The three mixtures abruptly increase Cs^{-1} and they have one or two maxima in the range between 0.4 and 0.9. Since the values determined from the steep slopes of π–A curves apparently involve experimental errors, the absolute values themselves should be excluded from detailed consideration; we can say at least that at the higher range of sterol mole fraction higher elasticity or lower compressibility is attained but distinction among three mixed systems is not clear enough so the results are not well ascribable to specialty of each molecular structure of the sterols.

As for the mechanical property of DPPC/Ch mixed monolayer, Chou and Chang have investigated the relaxation kinetics by measuring the surface area as a function of time at 37 °C and a constant surface pressure of 40 mN m^{-1}, showing that the relaxation process could be described by the models considering nucleation and growth mechanism [18]. Our investigation on the elastic property of DPPC/Ch monolayer was performed under conditions differing from 37 °C and 40 mN m^{-1}, nevertheless our results also seem to support their results and interpretation.

Table 5
Activity coefficients of 1 (DPPC) and 2 (Ch, Chsta, or Stig) as a function of X_{st} at discrete surface pressures

Mole fraction, X	Activity coefficients											
	$\pi = 5\,mN\,m^{-1}$		$\pi = 10\,mN\,m^{-1}$		$\pi = 15\,mN\,m^{-1}$		$\pi = 20\,mN\,m^{-1}$		$\pi = 25\,mN\,m^{-1}$		$\pi = 30\,mN\,m^{-1}$	
	f_1	f_2	f_1	f_2	f_1	f_2	f_1	f_2	f_1	f_2	f_1	f_2
(a) Ch												
0.0												
0.1	0.99	0.36	0.98	0.15	0.98	0.13	0.97	0.13	0.96	0.04	0.96	0.04
0.2	0.97	0.62	0.94	0.39	0.95	0.42	0.92	0.28	0.93	0.34	0.92	0.26
0.3	0.93	0.68	0.87	0.48	0.84	0.39	0.86	0.43	0.83	0.37	0.81	0.33
0.4	0.85	0.69	0.74	0.51	0.72	0.48	0.72	0.48	0.72	0.48	0.69	0.43
0.5	0.81	0.81	0.69	0.69	0.64	0.64	0.60	0.60	0.60	0.60	0.56	0.56
0.6	0.77	0.89	0.63	0.81	0.58	0.78	0.60	0.79	0.56	0.77	0.61	0.80
0.7	0.73	0.94	0.57	0.90	0.61	0.91	0.64	0.92	0.55	0.90	0.56	0.90
0.8	0.66	0.97	0.53	0.96	0.55	0.96	0.60	0.97	0.51	0.96	0.35	0.94
0.9	0.66	0.99	0.61	0.99	0.43	0.99	0.53	0.99	0.35	0.99	0.24	0.985
1.0												
(b) Chsta												
0.0												
0.1	0.99	0.55	0.98	0.21	0.99	0.39	0.98	0.19	0.98	0.20	0.97	0.07
0.2	0.97	0.62	0.94	0.39	0.95	0.42	0.92	0.28	0.93	0.34	0.92	0.26
0.3	0.95	0.74	0.86	0.45	0.84	0.38	0.86	0.43	0.87	0.48	0.84	0.39
0.4	0.86	0.72	0.76	0.54	0.75	0.52	0.72	0.48	0.72	0.48	0.71	0.46
0.5	0.81	0.81	0.68	0.68	0.66	0.66	0.61	0.61	0.66	0.66	0.58	0.58
0.6	0.75	0.88	0.63	0.82	0.60	0.80	0.55	0.76	0.60	0.80	0.56	0.77
0.7	0.80	0.96	0.63	0.92	0.65	0.92	0.55	0.90	0.75	0.95	0.57	0.90
0.8	0.74	0.98	0.55	0.96	0.53	0.96	0.42	0.95	0.75	0.98	0.55	0.96
0.9	0.72	1.00	0.62	0.99	0.41	0.99	0.26	0.98	0.78	1.00	0.52	0.99
1.0												
(c) Stig												
0.0												
0.1	1.00	0.60	0.99	0.32	0.98	0.19	0.99	0.37	0.99	0.33	0.97	0.07
0.2	0.97	0.63	0.95	0.44	0.94	0.38	0.94	0.39	0.93	0.33	0.93	0.30
0.3	0.92	0.62	0.87	0.47	0.84	0.39	0.88	0.48	0.84	0.39	0.84	0.38
0.4	0.90	0.79	0.80	0.60	0.78	0.57	0.75	0.52	0.77	0.56	0.78	0.56
0.5	0.82	0.82	0.73	0.73	0.71	0.71	0.68	0.68	0.64	0.64	0.61	0.61
0.6	0.78	0.90	0.64	0.82	0.63	0.82	0.58	0.79	0.58	0.78	0.55	0.77
0.7	0.72	0.94	0.62	0.92	0.59	0.91	0.63	0.92	0.61	0.91	0.58	0.91
0.8	0.82	0.99	0.70	0.98	0.61	0.97	0.71	0.98	0.77	0.98	0.70	0.98
0.9	0.79	1.00	0.65	0.99	0.71	1.00	0.52	0.99	0.39	0.99	0.62	0.99
1.0												

It should be noted that hysteresis phenomenon of π–A behavior which is characteristic to the lung surfactant was investigated by gradually increasing A, however, π was lowered along the π–A curves of the compression process, meaning that little hysteresis was observed. It may be necessary for a lung surfactant-like system to contain more prominently or widely changeable amphiphiles, with regard to the conformation at the air/water interface. Such as polypeptides the hydrophobic–hydrophilic balance of which is suitably designed so as to take to some extent a longer relaxation time will lead to a desirable hysteresis.

3.5. Phase diagram

In order to investigate the details in the composition dependence of monolayer properties, two-dimensional phase diagrams were constructed for the respective mixtures as shown in Fig. 7. The transition of DPPC-rich monolayer film was clearly observable up to $X_{st} = 0.2$ for all of the mixed system and the pressure slightly increased with increased composition of sterols; this is interpreted in terms of colligative properties. At the composition range higher than $X_{st} = 0.2$ the transition from LE to LC was not detectable. (For DPPC/Ch mixed monolayer at 37 °C no transition was seen [18]). On the other hand, the sudden break of π–A curves may be considered to result from the collapse phenomena of the monolayer films, as is well known. The pressure has been called ‘collapse pressure’ and examining the collapse pressure as a function of composition can give information on the mixing state of component molecules in a given mixed monolayer. Joos and Demel has derived the following equations on the basis of RST [35] and allowed us to widely apply the equations [36,37].

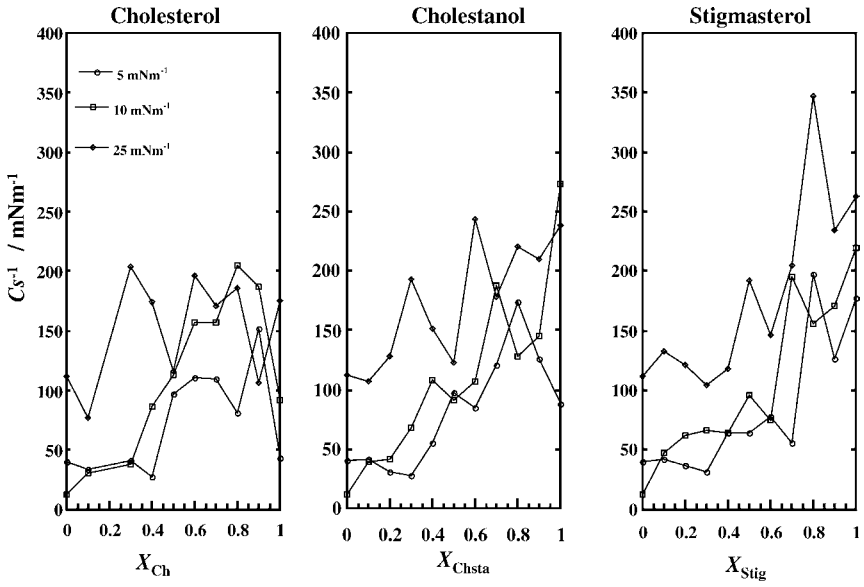

Fig. 6. Elasticity as a function of sterols mole fraction at 298 K.

$$1 = X_1^S f_1 \exp\left\{\frac{(\pi_{c,m} - \pi_{c,1})a_1}{k_B T}\right\} \exp\{\xi(X_2^S)^2\} + X_2^S f_2 \times \exp\left\{\frac{(\pi_{c,m} - \pi_{c,2})a_2}{k_B T}\right\} \exp\{\xi(X_1^S)^2\} \quad (9)$$

where X_1^S and X_2^S denote the mole fractions of components in the mixed monolayer film, respectively, π_1 and π_2 the respective collapse pressures, π_m the collapse pressure of mixed monolayer, a_1 and a_2, the respective surface area at the collapse pressure, ξ the interaction parameter, $k_B T$, the product of Boltzmann constant with the Kelvin temperature, and f_1 and f_2 are the respective surface activity coefficients at the collapse pressure.

In Eq. (9) when the activity coefficients, f_1 and f_2 are unity, the formed monolayer is considered to be of ideal mixing, and the curves calculated by applying Eq. (9) to ideal mixing are indicated by dotted lines in the respective mixed systems. The measured collapse pressures are plotted against mole fraction. For the mixed systems above $X_{st} = 0.4$, the collapse pressure of liquid condensed film could be comparatively easily determined, while, in the range being richer in DPPC, its determination was not definitely possible

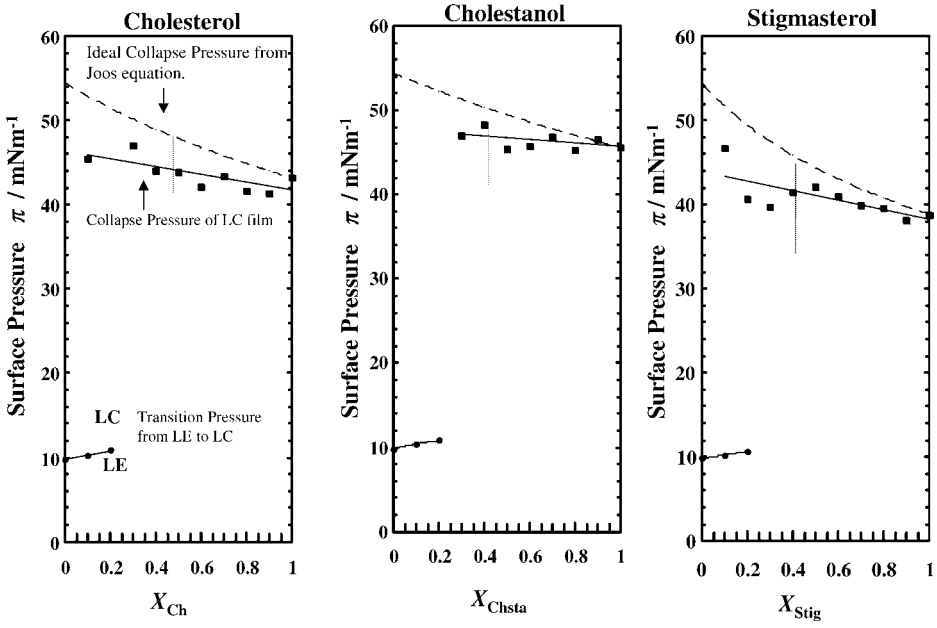

Fig. 7. Phase diagrams of the respective mixed systems at 298 K.

from the π–A curves. In the range above $X_{st} = 0.6$, the collapse pressure is likely to be constant or slightly go down as sterol composition increases.

In previous studies on monolayers formed by mixed system Ch with some species of bile acids (BAs) such as deoxycholic acid [36,38,39], tauro- and glyco-chonodeoxycholic acids and tauro- and chenodeoxycholic acids [40], Ch and BAs are found to be demixing in the monolayers films. This means that the lateral interaction between Ch and BAs (amongst BAs in particular deoxycholic acid) is extremely unfavorable and the lack of lateral interaction can explain why BAs are in general poor at solubilizing Ch [32]. Handa and Nakagaki [41] studied the miscibility of hexadecyl dihydrogen phosphate (HP) and Ch in a mixed monolayer spread on aqueous solution of HCl and HCl + urea. They found that the HP/Ch mixed system formed a "patched monolayer" in which the two components are demixed, and also that the addition of 4 M urea made the components miscible. Their results suggest that the interaction, including hydrogen bonding between hydrophilic groups, plays an important role in monolayer formation. In connection with miscibility or immiscibility in bulk and/or film phase Funasaki had theoretically shown a predicted phase as early as 1975 [42].

Here, again looking at the relations of molecular area with mole fraction, all the data above $\pi = 20\,\mathrm{mN\,m^{-1}}$ (see Fig. 4) are likely to exhibit an approximately linear relation which satisfies the additivity rule. This apparent satisfaction does not always mean ideal mixing occurs, because, even when a patched film (of complete demixing) is formed the additivity rule is satisfied. Considering the results described above, the present mixed systems of DPPC with three sterols may form a patched film in the higher surface pressure region, especially in the mixed systems containing sterols more than DPPC. In contrast, in mixed systems such as those composed of rich DPPC (major) and poor sterols (minor) there may exist to a partial extent a complex of DPPC molecules centering around a sterol molecule. Complex formation of phosphplipid with Ch has been suggested by Huang and Feigenson [43]. The extent of such a complex formation is not yet known, however, the great negative surface excess free energy suggests that a strong cohesive force acts between Ch, Chsta, or Stig and DPPC especially when sterol molecules are surrounded by DPPC molecules.

Recently, Hossain et al. [44,45] have studied extensively the phase transition of monolayers (Gibbs adsorption layers) of various single or mixed amphiphilic systems by using Brewster angle microscopy (BAM), in which they observed surface pressure change with time at different temperatures and in parallel they took BAM images. For instance, both first- and second-order phase transitions in the Gibbs adsorption layers of *n*-hexadecyl phosphate were clearly demonstrated with BAM [44], and a first order phase transition from a fluid like phase to a condensed phase was also observed in detail on the surface of a 1:1 binary mixed solution containing 2-hydroxyethyl laurate and either tetraoxa-octacosanoate or tetraoxa-triacontanoate [45]. Our observation only through π–A curves lacks detailed and definitive information on the transitions, however, if BAM were applied for observing condensed structure formation in the present mixed systems, a more comprehensive interpretation would have been derived. Application of such a method as BAM is a subject to be performed in near future.

Acknowledgements

This work was in part supported by funds from the Advanced Material Institute, Fukuoka University (Project II) and from the Fukuoka University Central Research Institute (No. 015004).

References

[1] A.W. Adamson, Physical Chemistry of Surfaces, fifth ed., Wiley, New York, 1990 (Chapter IV).
[2] G.L. Gaines Jr., J. Colloid Interface Sci. 21 (1996) 315.
[3] K.J. Bacon, G.T. Barnes, J. Colloid Interface Sci. 671 (1978) 70.
[4] H.E. Ries Jr., H. Swift, J. Colloid Interface Sci. 64 (1978) 111.
[5] D.A. Cadenhead, F. Müller-Landaw, Chem. Phys. Lipids 25 (1979) 329.
[6] K. Tajima, N.L. Gershfeld, Adv. Chem. 144 (1975) 165.
[7] L. Ter-Minassian-Saraga, J. Colloid Interface Sci. 70 (1979) 245.
[8] H. Matuo, N. Yoshida, K. Motomura, R. Matuura, Bull. Chem. Soc. Jpn. 52 (1979) 667.
[9] T.P.W. McMuller, R.N. Elhaney, Biochim. Biophys. Acta 1234 (1995) 90.
[10] K. Gong, S.-H. Feng, Colloids Surfaces A 207 (2002) 113.
[11] H.E. Ries Jr., Colloids Surf. A 10 (1984) 283.
[12] J.P. Slotte, Chem. Phys. Lipids 102 (1999) 13.
[13] P. Mattijus, J.P. Slottle, Chem. Phys. Lipids 81 (1996) 69.
[14] P. Mattijus, R. Bittman, C. Vilchèze, J.P. Slottle, Biochim. Biophys. Acta 1240 (1995) 237.
[15] H.M. McConnell, Annu. Rev. Phys. Chem. 42 (1991) 171.
[16] T.G. Anderson, H.M. McConnell, Colloids Surf. A: Physicochem. Eng. Aspects 171 (2002) 13.
[17] P. Dynarowicz-Latka, R. Seoane, J. Minones Jr., M. Velo, J. Minunes, Colloids Surf. B: Biointerf. 27 (2002) 249.
[18] T.-H. Chou, C.-H. Chang, Colloids Surf. B: Biointerf. 17 (2000) 71.
[19] S. Yamamoto, O. Shibata, S. Lee, G. Sugihara, Prog. Anesth. Mech. (special issue) 3 (1995) 25.
[20] Y. Tanaka, S. Lee, O. Shibata, G. Sugihara, The Ninth International Conference on Organized Molecular Films (LB9), vol. 1, 2000, p. 194.
[21] J.A. Whitsett, T.E. Weaver, in: J.R. Bourbon (Ed.), Pulmonary Surfactant: Biochemical, Fundamental, Regulatory and Clinical Concepts, CRC Press, Boston, 1991 (Chapter 4).
[22] R.J. King, J.A. Clements, Am. J. Physiol. 223 (1972) 727.
[23] S. Schürch, Respir. Physiol. 48 (1982) 339.
[24] H. Bachofen, S. Schürch, M. Urbinelli, E.R. Weibel, J. Appl. Physiol. 62 (1987) 1978.
[25] R.H. Notter, in: B. Robertson, L.M.G. van Golde, J.J. Batenburg Jr. (Eds.), Pulmonary Surfactant, Elsevier, New York, 1984 (Chapter 2).
[26] (a) I. Ikeda, K. Tanaka, M. Sugano, G.V. Vahouny, L.L. Gallo, J. Lipid Res. 29 (1988) 1573;
(b) I. Ikeda, K. Tanaka, M. Sugano, G.V. Vahouny, L.L. Gallo, J. Lipid Res. 29 (1988) 1583.
[27] S. Nagadome, Y. Okagaki, S. Lee, Y. Sasaki, G. Sugihara, Langmuir 17 (2001) 4405.

[28] A.-F. Mingotaud, C. Mingotaud, L.K. Petterson, Handbook of Monolayers, vols. 1 and 2, Academic Press, San Diego, 1993.
[29] R.H. Notter, S.A. Tabak, R.D. Mavis, J. Lipid Res. 21 (1980) 10.
[30] R.E. Pagano, N.L. Greshfeld, J. Phys. Chem. 76 (1972) 1238; R.E. Pagano, N.L. Gershfeld, J. Phys. Chem. 76 (1972) 1238.
[31] M. Senoo, Entropy, Kyouritu Shuppan, Tokyo, 1993, pp. 114–122.
[32] Y.M. Moroi, Plenum Press, New York, 1992 (Chapter 10).
[33] S. Nagadome, Y. Okazaki, S. Lee, Y. Sasaki, G. Sugihara, Langmuir 17 (2001) 4405–4412.
[34] N. Watanabe, A. Watanabe, Y. Tamai, Hyomen oyobi Kaimen (Surface and Interface), Kyouritsu Shuppan, Tokyo, 1973, pp. 58–60.
[35] P. Joos, R.A. Demel, Biochim. Biophys. Acta 183 (1969) 447.
[36] G. Sugihara, Y. Yamamoto, S.K. Yamamoto, S. Lee, Y. Sasaki, S. Nagadome, G. Sugihara, Colloid Surf. B: Biointerf. 6 (1996) 91–100.
[37] H. Miyosi, S. Nagadome, G. Sugihara, H. Kagimoto, Y. Ikawa, H. Igimi, O. Shibata, J. Colloid Interface Sci. 149 (1992) 216–225.
[38] S.K. Yamamoto, O. Shibata, M. Sakai, Y. Sasaki, S. Lee, G. Sugihara, Colloid Surf. B: Biointerf. 5 (1995) 249–253.
[39] G. Sugihara, S.K. Yamamoto, S. Nagadome, S. Lee, Y. Sasaki, O. Shibata, H. Igimi, Colloid Surf. B: Biointerf. 6 (1996) 81–89.
[40] (a) S. Nagadome, O. Numata, G. Sugihara, Y. Sasaki, H. Igami, Colloid Polym. Sci. 273 (1995) 675–680;
(b) S. Nagadome, H. Miyosi, G. Sugihara, H. Kagimoto, Y. Ikawa, H. Igimi, J. Jpn. Oil Chem. (Yakugaku) 39 (1990) 542.
[41] T. Handa, M. Nakagaki, Yakugaku Zassi 96 (1976) 912.
[42] N. Funasaki, Nippon Kagaku Kaishi (1975) 1841.
[43] J. Huang, G.W. Feigenson, Biophys. J. 76 (1999) 2142–2157.
[44] M.M. Hossain, T. Suzuki, T. Kato, Colloids Surf. A: Physicochem. Eng. Aspects 198–200 (2002) 53–57.
[45] M.M. Hossain, M.N. Islam, T. Okano, T. Kato, Colloids Surf. A: Physicochem. Eng. Aspects 205 (2002) 249–260.